UCRL- 83731
PREPRINT

THE MULTIBAND METHOD IN RADIATIVE TRANSFER CALCULATIONS

D. E. Cullen
G. C. Pomraning

This paper was prepared for submittal to
Journal of Quantitative Spectroscopy and
Radiative Transfer

December 1979

Lawrence Livermore Laboratory

This is a preprint of a paper intended for publication in a journal or proceedings. Since changes may be made before publication, this preprint is made available with the understanding that it will not be cited or reproduced without the permission of the author.

CIRCULATION COPY
SUBJECT TO RECALL
IN TWO WEEKS

DISCLAIMER

This document was prepared as an account of work sponsored by an agency of the United States Government. Neither the United States Government nor the University of California nor any of their employees, makes any warranty, express or implied, or assumes any legal liability or responsibility for the accuracy, completeness, or usefulness of any information, apparatus, product, or process disclosed, or represents that its use would not infringe privately owned rights. Reference herein to any specific commercial product, process, or service by trade name, trademark, manufacturer, or otherwise, does not necessarily constitute or imply its endorsement, recommendation, or favoring by the United States Government or the University of California. The views and opinions of authors expressed herein do not necessarily state or reflect those of the United States Government or the University of California, and shall not be used for advertising or product endorsement purposes.

THE MULTIBAND METHOD IN RADIATIVE TRANSFER CALCULATIONS

D. E. Cullen

and

G. C. Pomraning*

Lawrence Livermore Laboratory, University of California
Livermore, California 94550

ABSTRACT

The multiband method is developed for use in radiative transfer problems. The essence of the method is to divide the frequency range into both energy groups and cross section bands. Included in the formulation are the effects of continuously varying (in space and time) opacities, which leads to band-to-band streaming transfer terms. Several numerical examples indicate the increased accuracy possible by using a combination of groups and bands, as contrasted to groups alone.

---

*Permanent address: School of Engineering and Applied Science
University of California, Los Angeles
Los Angeles, CA 90024

1. Introduction

In multigroup transport or diffusion calculations, Nikolaev for neutrons[1] and Stewart for photons[2] originated the idea of within each group characterizing the neutrons or photons by the value of the total cross section with which they interact. The underlying idea of their approaches is to make full use of the predictions of various limiting transport problems. For example, in neutron transport the neutron flux varies inversely with total cross section in certain cases[3]. This known variation allows an accurate calculation of multigroup constants in these cases. Similarly, in photon transport (radiative transfer) Kirchhoff's law tells us that re-emission at any frequency is given by the product of the Planck distribution and the absorption cross section[4]. This implies that the Planck mean absorption coefficient is the proper mean in the emission dominated case.

Aspects of Nikolaev's and Stewart's work have been combined to develop the multiband method[5] which has been applied to a variety of neutron and photon problems[6]. In the usual multigroup method one can attempt to improve the transport model by using more energy groups. This is accomplished by further subdividing each energy interval. In the multigroup method neutrons or photons within each group all "see" or interact with the same total cross section. In the multiband method each group is further subdivided, not into smaller energy intervals, but rather into total cross section ranges. In this model neutrons or photons within each group can interact with more than one total cross section.

In this paper, the multiband equations, originally obtained and applied within the neutron transport context, are considered for

radiative transfer problems. Section 2 derives the multiband equations from one particular point of view in the simplest case of a medium whose cross sections are spatially independent (e.g., a homogeneous, constant temperature and pressure slab). The next section demonstrates that the required multiband parameters can be obtained from available multigroup photonics Planck and Rosseland mean opacities, which are the standard opacities now in use[4]. Section 4 considers a variety of simple problems to illustrate the differences that one obtains using the multiband method, compared to the usual multigroup method. Section 5 rederives the multiband equations from another point of view, including the generalization to spatially dependent cross sections (e.g., a multislab system with a temperature gradient). Continuous variations of cross sections, such as encountered in a strong temperature gradient, are much more extant in radiative transfer problems than in the neutron context. The paper concludes with a short section containing a few summary remarks.

2. The Multiband Equations in the Simplest Case

Consider the time dependent equation of radiative transfer (or neutron transport equation) which can be written in the form

$$\frac{1}{v}\frac{\partial I(\vec{r},E,\vec{\Omega},t)}{\partial t} + \vec{\Omega}\cdot\vec{\nabla}I(\vec{r},E,\vec{\Omega},t) + \Sigma_T(\vec{r},E,t)I(\vec{r},E,\vec{\Omega},t) = R(\vec{r},E,\vec{\Omega},t) \quad . \qquad (1)$$

Here R is the total source given by, in the most general case,

$$R(\vec{r},E,\vec{\Omega},t) = \int_0^\infty dE' \int_{4\pi} d\vec{\Omega}' \int dt' F(E',\vec{\Omega}',t' \to E,\vec{\Omega},t) \quad . \qquad (2)$$

The independent space, energy, angle, and time variables are denoted by $\vec{r}$, E, $\vec{\Omega}$, and t, and $I(\vec{r},E,\vec{\Omega},t)$ is the specific intensity of radiation (neutron angular flux). The particle speed is denoted by v (v = c = speed of light for photons), and $\Sigma_T(\vec{r},E,t)$ is the total collision cross section. The function $F(E',\vec{\Omega}',t' \to E,\vec{\Omega},t)$ is the transfer law, and written in this general way is meant to encompass scattering (including induced terms), delayed neutron production, fission, re-radiation, external sources, etc.

The multigroup equations are obtained from Eq. (1) by integration over adjacent energy (i.e., frequency in radiative transfer) intervals extending from E_g to E_{g+1}, g = 1, 2, ... G. This yields the coupled set of equations

$$\frac{1}{v_g}\frac{\partial I_g(\vec{r},\vec{\Omega},t)}{\partial t} + \vec{\Omega}\cdot\vec{\nabla}I_g(\vec{r},\vec{\Omega},t) + \Sigma_{Tg}(\vec{r},\vec{\Omega},t)I_g(\vec{r},\vec{\Omega},t) = R_g(\vec{r},\vec{\Omega},t) \quad , \qquad (3)$$

where I_g, R_g, or $\Sigma_{Tg}I_g$ is defined by integrating each of the corresponding energy dependent quantities over a group, e.g.,

$$I_g(\vec{r},\vec{\Omega},t) = \int_{E_g}^{E_{g+1}} dE I(\vec{r},E,\vec{\Omega},t) \quad . \tag{4}$$

The multiband equations are obtained in a similar manner by first multiplying Eq. (1) by a weight function

$$W \equiv \delta \left[\Sigma_T(E) - \Sigma_T^* \right] \quad , \tag{5}$$

and then integrating Eq. (1) over both an energy range and a total cross section range, with respect to Σ_T^*. The result is a set of coupled equations

$$\frac{1}{v_g} \frac{\partial I_{gb}(\vec{r},\vec{\Omega},t)}{\partial t} + \vec{\Omega}\cdot\vec{\nabla} I_{gb}(\vec{r},\vec{\Omega},t) + \Sigma_{Tgb}(\vec{r},\vec{\Omega},t) = R_{gb}(\vec{r},\vec{\Omega},t) \quad , \tag{6}$$

where I_{gb}, R_{gb}, or $\Sigma_{Tgb} I_{gb}$ is defined by integrating each of the corresponding energy dependent quantities over an energy group and total cross section band, e.g.,

$$I_{gb}(\vec{r},\vec{\Omega},t) = \int_{\Sigma_{Tgb}}^{\Sigma_{Tg,b+1}} d\Sigma_T^* \int_{E_g}^{E_{g+1}} dE \delta\left[\Sigma_T(E) - \Sigma_T^*\right] I(\vec{r},E,\vec{\Omega},t) \quad . \tag{7}$$

Physically, the effect of the delta function is to only select those energy intervals in the group within which the total cross section is between Σ_{Tgb} and $\Sigma_{Tg,b+1}$. Therefore this integral is equivalent to collecting together all those particles in a given energy interval (E_g, E_{g+1}) that interact with a given range of total cross sections (Σ_{Tgb}, $E_{Tg,b+1}$).

Figures 1 through 3 illustrate the procedures involved in dividing an energy group (E_g, E_{g+1}) into four total cross section bands. In figure 1

the total cross section between energies E_g and E_{g+1} is illustrated. In addition, in this figure the total cross section range is divided into four subranges, or bands. In figure 2 we illustrate the effect of applying Eq. (7) to the third band. The effect of the Dirac delta function and integration over a band of total cross section in Eq. (7) is that there will only be non-zero contributions to the integral from those energy ranges in which the total cross section is in the range Σ_{T3} to Σ_{T4}. The contributing energy intervals are illustrated in figure 2 by the dark areas. The multiband method is thus equivalent to collecting together all energy intervals in which the total cross section is in a given range, as illustrated in figure 3, and applying the usual multigroup method to this reordered total cross section. In this figure, x is a normalized, rearranged energy variable. Each of these bands is then characterized by average cross sections to define the parameters in Eq. (6).

It is important to realize that the multigroup equations [see Eq. (3)] and the multiband equations [see Eq. (6)] are identical in form and differ only in the magnitude of the parameters, such as Σ_{Tg} versus Σ_{Tgb}. Therefore, in principle once these parameters are defined the multiband equations can be solved by existing multigroup radiative transfer or neutron transport codes. Once the multiband equations have been solved to define the specific intensity of radiation (neutron flux) in each band, the equivalent multigroup quantities can be obtained by simply adding up the contributions from all bands within each group,

$$I_g(\vec{r},\vec{\Omega},t) = \sum_b I_{gb}(\vec{r},\vec{\Omega},t) \quad . \tag{8}$$

One important characteristic of the multiband method is that if we define the equivalent multigroup total cross section in the normal manner as the ratio of collisions to radiative intensity (neutron flux), i.e.,

$$\Sigma_{Tg} = \frac{\sum_b \Sigma_{Tgb} I_{gb}(\vec{r},\vec{\Omega},t)}{\sum_b I_{gb}(\vec{r},\vec{\Omega},t)} , \qquad (9)$$

we can see that even starting from spatially independent multiband cross sections Σ_{Tgb}, the equivalent multigroup cross section Σ_{Tg} may be spatially, angular, and time dependent due to the variation in the radiative intensity (neutron flux) within each cross section band. The importance of this effect will be illustrated in Section 4.

3. The Multiband Parameters

The direct use of Eq. (7) to define multiband parameters would be complicated and expensive. However, there is a simple procedure that may be used to derive the required multiband parameters directly from existing library data, such as Planckian and Rosseland means. In order to accomplish this we will first illustrate that the normal definition of multigroup cross sections in terms of an integral over energy can be exactly transformed into an integral over total cross section. This point is not surprising since it merely illustrates that one can either integrate over the energy interval in the Riemann sense, or over the total cross section range in the Lebesque sense. However, it will introduce the concept of a band weight or probability.

Consider the definition of a multigroup cross section, i.e.,

$$\Sigma_{ig} = \frac{\int_{E_g}^{E_{g+1}} dE \Sigma_i(E) I(\vec{r},E,\vec{\Omega},t)}{\int_{E_g}^{E_{g+1}} dE\ I(r,E,\vec{\Omega},t)} \quad , \tag{10}$$

where $\Sigma_i(E)$ is the cross section for the i^{th} interaction (e.g., scattering, absorption, etc.), and $I(\vec{r},E,\vec{\Omega},t)$ is the weighting function which approximates the specific intensity of radiation (neutron flux). The weighting function used in photon and neutron transport calculations is usually written as the product of two terms,

$$I(\vec{r},\vec{\Omega},E,t) = S(E)W(\Sigma_T) \quad , \tag{11}$$

where S(E) is the energy dependent "envelope" of the weight function, and $W(\Sigma_T)$ is a cross section dependent self-shielding factor. Specifically, for photons and neutrons the weighting functions most often used are shown in Table 1. In this table, M(E) is the neutron energy dependent envelope function which is a composite Maxwellian, 1/E, and fission or fusion spectra[7]; $B_\nu(T)$ is the blackbody distribution[4], Σ_T is the total cross section, Σ_o is a cross section representing effects of other materials and spatial leakage, and N is an integer which indicates the angular Legendre component of the neutron flux being considered. From this table it may be seen that unshielded neutron cross sections are analogous to Planckian mean cross sections for photons, in the sense that both use the same self-shielding factor (W = 1). Similarly, the totally self-shielded neutron cross sections (Σ_o = 0, N = 1) are analogous to Rosseland mean cross sections for photons, in the sense that both use the same self-shielding factor ($W = 1/\Sigma_T$). Without introducing the concept of self-shielding, the two extremes of unshielded/Planckian on the one hand and totally shielded/Rosseland cross sections on the other hand can be shown to be equivalent to conserving either reaction rates or distance to collision, respectively.

In the following development, it is assumed that the weighting function is separable according to Eq. (11). However, it is fairly straightforward to show that the following results apply to any weighting function; the separable function is used to simplify the following derivations and to illustrate how this approach directly applies to the weighting functions normally used to define photon and neutron multigroup cross sections. The definition of the multigroup cross section, Eq. (10), may be written in the equivalent form

$$\Sigma_{ig} = \frac{\int_{E_g}^{E_{g+1}} dE \int d\Sigma_T^* \delta \left[\Sigma_T^* - \Sigma_T(E) \right] \Sigma_i(E) S(E) W(\Sigma_T^*)}{\int_{E_g}^{E_{g+1}} dE \int d\Sigma_T^* \delta \left[\Sigma_T^* - \Sigma_T(E) \right] S(E) W(\Sigma_T^*)} \quad . \tag{12}$$

If the integrations over Σ_T^* are performed first we return to the normal definition of the group averaged cross section, given by Eq. (10). However, if the integrations over E are performed first we obtain the equivalent equation

$$\Sigma_{ig} = \frac{\int d\Sigma_T^* \Sigma_i(\Sigma_T^*) W(\Sigma_T^*) p(\Sigma_T^*)}{\int d\Sigma_T^* W(\Sigma_T^*) p(\Sigma_T^*)} \quad , \tag{13}$$

where we have defined

$$p(\Sigma_T^*) = \frac{\int_{E_g}^{E_{g+1}} dE \delta \left[\Sigma_T^* - \Sigma_T(E) \right] S(E)}{\int_{E_g}^{E_{g+1}} dE S(E)} \quad , \tag{14}$$

$$\Sigma_i(\Sigma_T^*) p(\Sigma_T^*) = \int_{E_g}^{E_{g+1}} dE \delta \left[\Sigma_T^* - \Sigma_T(E) \right] \Sigma_i(E) S(E) \quad . \tag{15}$$

Equations (14) and (15) serve to define the total cross section probability density, $p(\Sigma_T^*)$, and the cross section for each reaction i as a function of the total cross section, $\Sigma_i(\Sigma_T^*)$. From its definition, it can be seen that $p(\Sigma_T^*)d\Sigma_T^*$ is roughly a normalized probability distribution that defines the probability of the total cross section being within $d\Sigma_T^*$ of Σ_T^* within the energy interval (E_g, E_{g+1}). This interpretation of $p(\Sigma_T^*)$ would be precise if S(E) = 1. It is important to realize that since the definition of the group averaged cross section as an integral over the total cross section [see Eq. (13)] has been derived from the usual definition over energy [see Eq. (10)] merely by introducing definitions, but no approximations, the two forms are exactly equivalent.

The advantage of using the cross section dependent form to define group averaged cross sections according to Eq. (13) may be demonstrated by comparing the relative difficulty of evaluating the two integrals appropriate to the neutron problem

$$I_1 \equiv \int_{E_g}^{E_{g+1}} dE \, \frac{1}{E\left[\Sigma_T(E) + \Sigma_o\right]} \quad , \tag{16}$$

and

$$I_2 \equiv \int_{\Sigma_{Tmin}}^{\Sigma_{Tmax}} d\Sigma_T^* \, \frac{p(\Sigma_T^*)}{\left[\Sigma_T^* + \Sigma_o\right]} = \int_0^1 dP \frac{1}{\left[\Sigma_T^*(P) + \Sigma_o\right]} \quad , \tag{17}$$

where in this example $p(\Sigma_T^*)$ is given by Eq. (14) with $S(E) = 1/E$. As a concrete example, we consider the Pu - 239 cross sections between 40 and 300 ev. Figure 4 showns these microscopic cross sections in barns (b), and it is clear that in the energy-cross section plane $\Sigma_T(E) + \Sigma_o$ is a rapidly varying, fairly complicated function represented by thousands of data points. By contrast, we see in Figure 5 that in the probability-cross section plane $\Sigma_T^* + \Sigma_o$ would be a simple monotonically increasing function of P. Therefore, once the total cross section probability density is known, integrals in the probability versus cross section plane may be performed very efficiently for a variety of self-shielding functions, $W(\Sigma_T^*)$. Another advantage of using the probability versus cross section plane is the increased physical insight that is obtained by allowing one to examine the importance of specific cross section ranges [see Fig. 5] instead of having to deal with hundreds of cross section minima and maxima. Although the above example is drawn from neutron transport, the same considerations may be even more important in radiative transfer involving lines. Radiative transfer lines can be narrower and more numerous than neutron resonances.

In order to define the multiband parameters the exact definition of the multigroup cross section, Eq. (13), as an integral over the total cross section range is replaced by a quadrature, i.e.,

$$\Sigma_{ig} = \frac{\sum_b \Sigma_{ib} W(\Sigma_{Tb}) p_b}{\sum_b W(\Sigma_{Tb}) p_b} \quad . \tag{18}$$

This is of course equivalent to representing the total cross section probability $p(\Sigma_T^*)$ by a set of Dirac delta functions

$$p(\Sigma_T^*) = \sum_b P_b \delta \left[\Sigma_T^* - \Sigma_{Tb} \right] \quad . \tag{19}$$

Once the band weights p_b are known, they may be used in Eq. (18) with any weighting function $W(\Sigma_T)$ to define group averaged cross sections, Σ_{ig}.

However, we will use the reverse procedure. If we know a set of group averaged cross sections obtained by using a variety of weighting functions $W(\Sigma_T)$, Eq. (18) may be solved to define the band weights p_b and cross sections Σ_{ib}. This is the procedure that we shall use here to define multiband parameters. Specifically, if we are given $\Sigma_i(W_\ell)$ and W_ℓ, $\ell = 0, 1, 2, \ldots$. for a given group, we then must solve the set of equations

$$\Sigma_i(W_\ell) = \frac{\sum_b \Sigma_{ib} W_\ell(\Sigma_{Tb}) p_b}{\sum_b W_\ell(\Sigma_{Tb}) p_b} \quad , \qquad \ell = 0, 1, 2, \ldots . \tag{20}$$

to define Σ_{ib} and p_b, $b = 1, 2, \ldots$. This is a classical moments problem. Specifically, if we use

$$W_\ell(\Sigma_T) = 1/\Sigma_T^\ell \quad , \qquad \ell = 0, 1, 2, \ldots . \tag{21}$$

this problem becomes a Hausdorff moments problem[8].

The simplest illustration of this procedure to consider two bands and apriori fix the band weights and solve for the band cross sections Σ_{T1} and Σ_{T2}.

Since in general there is no reason to do otherwise, we use equal band weights ($p_1 = p_2 = 1/2$). We assume that the Planckian and Rosseland group cross sections are known. Applying Eq. (20) then gives the two equations

$$\Sigma_P = \frac{1}{2}\left(\Sigma_{T1} + \Sigma_{T2}\right) \quad , \tag{22}$$

$$\Sigma_R = \left[\frac{1}{2}\left(\frac{1}{\Sigma_{T1}} + \frac{1}{\Sigma_{T2}}\right)\right]^{-1} \quad , \tag{23}$$

where Σ_P and Σ_R are the Planckian and Rosseland means, respectively. Solving for Σ_{T1} and Σ_{T2} gives the simple results[9]

$$\Sigma_{T1} = \Sigma_P\left[1 - \left(1 - \frac{\Sigma_R}{\Sigma_P}\right)^{1/2}\right] \quad , \tag{24}$$

$$\Sigma_{T2} = \Sigma_P\left[1 + \left(1 - \frac{\Sigma_R}{\Sigma_P}\right)^{1/2}\right] \quad . \tag{25}$$

If these two band parameters are used, one is guaranteed to obtain the correct solution in both the Planck and Rosseland limits, i.e., in the optically thin (emission dominated) and optically thick (near equilibrium) situations. However, away from these limiting situations, numerical calculations indicate that the 2-band, G group method is not substantially better than the 2G group method. It appears that the apriori assignment of equal weights is too restrictive.

According,it appears that for the multiband method to acheive its full potential, the weights for the two bands must also be treated as variables. This allows us to conserve an additional cross section, which

we somewhat arbitrarily take to be the so-called "super-Rosseland", or $1/\Sigma_T^2$ weighted cross section. This choice leads to very good numerical results, examples of which are discussed in the next section. In this scheme then, we solve for the two band parameters using the weighting functions and multigroup cross sections given in Table II. We obviously have four unknown parameters Σ_{T1}, Σ_{T2}, p_1, and p_2, and we require four equations to uniquely define these parameters. These are:

$$1 = p_1 + p_2, \text{(a normalized distribution)} \quad , \tag{26}$$

$$\Sigma_P = \frac{\Sigma_{T1}p_1 + \Sigma_{T2}p_2}{p_1 + p_2} \quad , \quad \text{(conservation of Planck mean)} \quad , \tag{27}$$

$$\Sigma_R = \frac{p_1 + p_2}{\frac{p_1}{\Sigma_{T1}} + \frac{p_2}{\Sigma_{T2}}} \quad , \quad \text{(conservation of Rosseland mean)} \quad , \tag{28}$$

$$\Sigma_S = \frac{\frac{p_1}{\Sigma_{T1}} + \frac{p_2}{\Sigma_{T2}}}{\frac{p_1}{\Sigma_{T1}^2} + \frac{p_2}{\Sigma_{T2}^2}} \quad , \quad \text{(conservation of super-Rosseland mean)} \quad . \tag{29}$$

Here Σ_S is the super-Rosseland mean, and Σ_P and Σ_R are as previously defined.

By inspection of Eqs. (26) through (29) we can see that the parameters are not uniquely defined. That is, we may exchange the parameters for the two bands and still obtain a solution. The parameters do not become unique until we introduce an ordering into the parameters, such as $\Sigma_{T1} < \Sigma_{T2}$. This leads us to believe that the two band parameters will be related to the roots of a quadratic equation. We make the change of variables

$$p_1 = \frac{1}{2} + \delta \quad , \qquad \Sigma_{T1} = \frac{1}{X_1} = \frac{1}{A + B} \quad , \tag{30}$$

$$p_2 = \frac{1}{2} - \delta \quad , \qquad \Sigma_{T2} = \frac{1}{X_2} = \frac{1}{A - B} \quad . \tag{31}$$

This change of variables immediately satisfies our first equation, and the remaining three equations may be solved to find

$$\delta = \frac{1 - A\Sigma_R}{2B\Sigma_R} \quad , \tag{32}$$

$$A = \frac{1}{2\Sigma_S}\left[\frac{\Sigma_P - \Sigma_S}{\Sigma_P - \Sigma_R}\right] \quad , \tag{33}$$

$$B^2 = \frac{1}{\Sigma_R\Sigma_P}\left[1 - 2A\Sigma_R + \Sigma_R\Sigma_P A^2\right] \quad . \tag{34}$$

As expected, there are two possible solutions for B, corresponding to the positive and negative roots of B^2. This is the result of the non-uniqueness of the solution without an ordering. From the definition of X_1, X_2, and δ in terms of B, it may be seen that choosing the positive or negative value of B yields the same two band weights and band cross sections with the pairs (p_1, Σ_{T1}) and (p_2, Σ_{T2}) exchanged. From the definitions of X_1, X_2, Σ_{T1}, and Σ_{T2}, choosing B positive corresponds to introducing an order such that $\Sigma_{T1} < \Sigma_{T2}$. The above algorithm will always produce physically acceptable parameters (positive band weights and band cross sections) as long as

$$\Sigma_P > \Sigma_R > \Sigma_S \quad . \tag{35}$$

The only time this inequality is not satisfied is when the cross section is independent of energy across the group[6]. In this case, of course, only one band is needed in the group, or both band cross sections are set equal to the energy independent value.

All of the parameters required to define two band cross sections and weights have now been uniquely defined in terms of the Planckian, Rosseland, and super-Rosseland cross sections for each group. The significance of using these three cross sections may be appreciated by comparing Eqs. (9) and (20). If, in fact, the radiative intensity is equal to the weighting function, i.e.,

$$I_{gb} = p_b/\Sigma_{Tb}^{\ell} \quad , \qquad \ell = 0,\ 1,\ 2 \quad , \tag{36}$$

the equivalent group averaged cross section will be the Planckian ($\ell = 0$), Rosseland ($\ell = 1$), or super-Rosseland ($\ell = 2$) mean. In particular, this implies, and it will be illustrated later, that the effect of explicitly conserving the cross sections in these limiting cases is that for optically thin media the equivalent group averaged cross section will reduce to the Planckian average, and in a near equilibrium thick medium it will reduce to the Rosseland average. For intermediate cases, the group average will slide between these two extremes.

4. Numerical Examples

In order to illustrate the effect of using two band cross sections instead of Rosseland or Planckian means, we first consider the results for a simple one group problem of radiation impinging upon a totally absorbing (no re-emission) halfspace, as shown schematically in figure 6. In this case the equation to solve is

$$\mu \frac{\partial N(x,E,\mu)}{\partial x} + \Sigma_T(E) N(x,E,\mu) = 0 \quad , \tag{37}$$

with the intensity N specified at x=0, i.e.,

$$N(0,E,\mu) = S(E,\mu). \tag{38}$$

The exact solution is, of course, exponential attenuation independently at each energy. We take the source $S(E,\mu)$ to be independent of energy, and a beam perpendicular to the surface, and normalized to one "particle" incident per unit time and area.

For this source, the contribution of any energy to the integral of $N(x,E,\mu)$ over energy at any point x depends only upon the total cross section $\Sigma_T(E)$. This cross section will be assumed to have a simple linear variation across the energy range of interest, with

$$\Sigma_T(E_g) = 10 \quad ; \; \Sigma_T(E_{g+1}) = 0.1 \tag{39}$$

It should be emphasized, however, that the solution will be the same for any cross section which has the same cross section probability density as that corresponding to Eq. (39). For example, the solution for each of the total cross sections variations shown in Figure 7 will be identical.

Figures 8 and 9 illustrate the results of an exact calculation compared to using Planckian, Rosseland, and two-band calculations for the photon intensity

$$N_o(x) \equiv \int_{-1}^{1} d\mu\mu \int_{E_g}^{E_{g+1}} dE N(x,E,\mu) = \int_{E_g}^{E_{g+1}} dE \exp[-\Sigma_T(E)x], \tag{40}$$

and the absorption or reaction rate

$$\begin{aligned} R_o(x) &\equiv \int_{-1}^{1} d\mu\mu \int_{E_g}^{E_{g+1}} dE \Sigma_T(E) N(x,E,\mu) \\ &= \int_{E_g}^{E_{g+1}} dE \, \Sigma_T(E) \exp[-\Sigma_T(E)x] . \end{aligned} \tag{41}$$

From Figure 8 we can see that the Planckian intensity rapidly deviates from the exact solution. The Rosseland intensity stays close to the exact solution deeper into the medium than the Planckian, but eventually it too deviates from the exact solution. By comparison, the two band solution approximates the exact solution quite well over the entire range of x shown in Figure 8.

From Figure 9 we can see one of the problems associated with using a Rosseland mean. At x=0, by taking the ratio of Eqs. (40) and (41), we may see that the exact group averaged cross section is the Planckian average. The use of the Rosseland average allows the radiation to propogate further into the medium [see Fig. 8] by reducing the cross section and therefore the reaction rate for the group. In the case presented here Figure 9 illustrates that the effect of using the Rosseland average is to lower the absorption or reaction rate by a factor of two at the point of highest reaction rate, x=0.

In this example we are being somewhat unfair to the Planckian and Rosseland solutions by comparing to a two band solution, since the two band solution is equivalent to solving two equations. Furthermore, none

of the methods exactly reproduce the exact answer. It is reasonable to inquire as to what happens if we subdivide the energy interval E_g to E_{g+1} into successively more groups. For a fair comparison we will use the same number of equations for each method; e.g., we will compare a 10 group, 2 band solution to a 20 group Rosseland or Planckian solution. Figure 10 illustrates the results obtained for each method by using progressively more equations. In this figure for each method the ratio of the approximate to the exact solution at x=0 is plotted versus the number of equations used. From Figure 10 we can see that in order to obtain a solution using Planckian or Rosseland averages to the same accuracy as a two band solution, one needs to use an order of magnitude more equations. In particular, the dotted line in this figure shows that a 1 group, 2 band solution is comparable in accuracy to a 40 group Planckian calculation. (For a Rosseland calculation, about 25 groups is required). This is a characteristic that the two band solution exhibits in many applications; the two band solution can be very accurate using only a few groups.

In the opposite extreme to the case just considered we may investigate what happens in a purely scattering (total re-emission) medium. In this case we will consider a steady state problem with isotropic radiation impinging upon a plane slab of thickness x, as shown schematically in Figure 11. By conservation, the incident radiation will either be transmitted through the slab or reflected since no radiation is absorbed. Figure 12 presents the results obtained for the transmission and albedo as the slab which is varied between 0.01 and 1000 Planckian mean free paths. For this example the Rosseland mean was assumed to be 0.1 times the Planckian mean. What we expect is that for optically thin slabs the

solution will be that corresponding to the use of Planckian means, and for thick slabs that corresponding to the use of Rosseland means. Figure 12 clearly illustrates this characteristic of the two band method; it smoothly slides between the Planckian and Rosseland correct limiting cases.

5. The Multiband Equation in the General Case

In deriving the multiband equations as given by Eq. (6), we have tacitly assumed that the total cross section, and hence the band parameters, are independent of space and time. More specifically, the limits on the Σ_T^* integrations in definitions such as Eq. (7) were assumed constant. This allowed the cross section integration to be passed through the space and time derivatives in the equation of transfer. If the total cross section is not constant in space and time, due to temperature and/or pressure gradients, the multiband equations are somewhat more complex. In particular, an additional term, representing streaming band to band transfer, is present. In this section, we reformulate the multiband method to include this effect. We also discuss the conditions to be applied at an interface between two similar, as well as two dissimilar, materials.

To provide an alternative to Section 2, our approach here will be less formal and more concrete. For this reason, as well as for simplicity, we deal with the simplest time independent equation of transfer,

$$\frac{\partial I(s,\nu)}{\partial s} = -\Sigma_T(s,\nu)\ [I(s,\nu) - B(\nu)] \quad , \tag{42}$$

where ν is the photon frequency ($E = h\nu$), s is the spatial variable along the photon flight direction, and B is the Planck function. Generalization of what follows to time dependence and a general source term is in Eq. (1) presents no problem. We also, for simplicity of presentation, restrict the discussion to the two band method.

In the two band formulation, we envision a cross section behavior between the group limits ν_g and ν_{g+1} as shown in Figure 13. In this

figure we have denoted the frequency at the right edge of the i^{th} "line" by an odd index (2i+1) and denoted the left edge by an even index (2i). We define the fractional measure of the low cross section (Σ_{T1}) as p_1, given by

$$p_1 = \frac{1}{\Delta\nu}\sum_i (\nu_{2i} - \nu_{2i-1}) , \tag{43}$$

where $\Delta\nu \equiv \nu_{g+1} - \nu_g$. Similarly, the fractional measure of the high opacity is defined to be p_2 and given by

$$p_2 \equiv \frac{1}{\Delta\nu}\sum_i (\nu_{2i+1} - \nu_{2i}) . \tag{44}$$

Clearly $p_1+p_2 = 1$. We define the corresponding band intensities as

$$I_1(s) \equiv \sum_i \int_{\nu_{2i-1}}^{\nu_{2i}} d\nu\, I(s,\nu) , \tag{45}$$

$$I_2(s) \equiv \sum_i \int_{\nu_{2i}}^{\nu_{2i+1}} d\nu I(s,\nu) . \tag{46}$$

To form the first band equation for $I_1(s)$, we integrate Eq.(42) over the first band (those frequencies corresponding to Σ_{T1}) to get

$$\sum_i \int_{\nu_{2i-1}}^{\nu_{2i}} d\nu \frac{\partial I(s,\nu)}{\partial s} = -\Sigma_{T1}(s)\left[I_1(s) - p_1(s) b \frac{acT^4}{4\pi}\right] , \tag{47}$$

where

$$b \equiv \frac{4\pi}{acT^4} \int_{\nu_g}^{\nu_{g+1}} d\nu B(\nu) \quad . \tag{48}$$

Physically, b is the fraction of the energy in a black body spectrum contained in the group under consideration. In obtaining the last term in Eq.(47) an assumption has been made that the "lines" are randomly distributed over the group, or alternately, that the group is narrow enough so that $B(\nu)$ does not vary appreciably over the group. To properly interchange the orders of integration and differentiation in Eq.(47), we need take into account that ν_{2i} and ν_{2i-1} depend upon s. We then obtain

$$\frac{\partial I_1(s)}{\partial s} - \sum_i \left[I(s,\nu_{2i}) \frac{\partial \nu_{2i}}{\partial s} - I(s,\nu_{2i-1}) \frac{\partial \nu_{2i-1}}{\partial s} \right] =$$

$$= -\Sigma_{T1}(s) \left[I_1(s) - p_1(s) \frac{acT^4}{4\pi} \right] \quad . \tag{49}$$

A similar development for the second band leads to the result

$$\frac{\partial I_2(s)}{\partial s} - \sum_i \left[I(s,\nu_{2i+1}) \frac{\partial \nu_{2i+1}}{\partial s} - I(s,\nu_{2i}) \frac{\partial \nu_{2i}}{\partial s} \right] =$$

$$= -\Sigma_{T2}(s) \left[I_2(s) - p_2(s) b \frac{acT^4}{4\pi} \right] \quad . \tag{50}$$

It remains to specify $I(s,\nu_i)$, the radiative density at the line edges. The term involving these densities in Eqs. (49) and (50) represent the transfer between bands as the photons stream. Clearly if we add Eqs.(49) and (50) these terms cancel, which is just a manifestation of the fact that a loss from one band is a gain to the other. That is,

streaming removes no photons from the group—it only rearranges the photons between bands. To specify $I(s,\nu_i)$, we proceed as follows. We begin by treating transport within a given material, in which the cross section is a function of temperature and pressure. The cross section at position s is "correlated" to the cross section at s+ds in the sense that a temperature and/or pressure gradient will broaden or sharpen the lines, but the line positions will not abruptly change. That is, in a given material the cross section is a continuous function of s if the temperature and pressure are continuous. In the two band model, the temperature and pressure s dependences give rise to the s dependence of the ν_i. We assume that a given change in temperature and pressure affects all of the lines the same; i.e., all lines either broaden or sharpen. For concreteness, let us assume that in going from position s to position s+ds that the temperature and pressure changes are such that all lines sharpen. This implies

$$\frac{\partial}{\partial s}(\nu_{2i} - \nu_{2i-1}) > 0, \text{ all } i, \tag{51}$$

and hence from Eq.(43) we see

$$\frac{\partial p_1}{\partial s} > 0 . \tag{52}$$

Since all lines act alike, we can for simplicity draw a picture for a single line as in Figure 14. The solid line gives $\Sigma_T(s,\nu)$ at s, and the dotted line shows the sharpening that occurs at s+ds. From this picture we see that a portion of the intensity from band 2 has been transferred to band 1, since band 2 is now smaller. That is, a part of what was in band 2 at s now finds itself in band 1 at s+ds. Hence the

proper density $I(s,\nu_i)$ to use in Eqs.(49) and (50) is the band 2 intensity since it is that which is transferred. Accordingly, for $\partial p_1/\partial s > 0$, we should use

$$I(s,\nu_i) = \frac{I_2(s)}{p_2(s)\Delta\nu} , \tag{53}$$

in which case Eqs. (49) and (50) become

$$\frac{\partial I_1(s)}{\partial s} - \frac{I_2(s)}{p_2(s)} \frac{\partial p_1(s)}{\partial s} = -\Sigma_{T1}(s)[I_1(s)-p_1(s)b \frac{acT^4}{4\pi}] , \tag{54}$$

$$\frac{\partial I_2(s)}{\partial s} - \frac{I_2(s)}{p_2(s)} \frac{\partial p_2(s)}{\partial s} = -\Sigma_{T2}(s)[I_2(s)-p_2(s)b \frac{acT^4}{4\pi}] . \tag{55}$$

Equations (54) and (55) are the two band equations. It must be emphasized that these equations only hold for $\partial p_1(s)/\partial s > 0$ within a given material. We shall shortly write down the corresponding equations for $\partial p_1(s)/\partial s < 0$, and later on we will consider what happens at an interface between materials. We note that the two band equations are formally identical to the usual two group equations, with an additional term in each equation accounting for transfer between bands.

One can ask what happens to the band intensities at discontinuity in p_1 and p_2, due to a discontinuity at temperature and/or pressure in a given material. To determine this, we rewrite Eq. (55) as

$$\frac{\partial}{\partial s}\left(\frac{I_2}{p_2}\right) = -\frac{\Sigma_{T2}}{p_2}[I_2-p_2 b \frac{acT^4}{4\pi}] , \tag{56}$$

and add Eqs. (54) and (55) to obtain

$$\frac{\partial}{\partial s}(I_1+I_2) = -\Sigma_{T1}(I_1-p_1 b \frac{acT^4}{4\pi}] - \Sigma_{T2}[I_2-p_2 b \frac{acT^4}{4\pi}] . \tag{57}$$

Integrating Eqs. (56) and (57) across the discontinuity, we find

$$\left(\frac{I_2}{p_2}\right)^- = \left(\frac{I_2}{p_2}\right)^+ \; ; \quad (I_1+I_2)^- = (I_1+I_2)^+ \; , \tag{58}$$

where - and + refer to the left and right, respectively, of the discontinuity. That is, the band 2 density $(I_2/p_2\Delta\nu)$ and the total intensity (I_1+I_2) are continuous across a discontinuity in p_1 and p_2. Again, we emphasize that this result corresponds to a discontinuity in p_1 and p_2 within a given material and for $\partial p_1/\partial s > 0$, i.e., $p_1^+ > p_1^-$.

Equation (58) suggests that the band 2 equation may be simpler if written in terms of the density rather than intensity. We define

$$\psi_1 \equiv I_1/p_1 \; ; \quad \psi_2 \equiv I_2/p_2 \; . \tag{59}$$

In terms of these variables, Eqs. (54) and (55), the two band equations, become

$$\frac{\partial\psi_1}{\partial s} + \frac{1}{p_1}(\psi_1-\psi_2)\frac{\partial p_1}{\partial s} = -\Sigma_{T1}\left[\psi_1 - b\,\frac{acT^4}{4\pi}\right] \; , \tag{60}$$

$$\frac{\partial\psi_2}{\partial s} = -\Sigma_{T2}\left[\psi_2 - b\,\frac{acT^4}{4\pi}\right] \; . \tag{61}$$

Equations (60) and (61) are the two band equations written in terms of densities. We note that the equation for ψ_2, Eq. (61), contains no reference to ψ_1.

All of our results have been obtained under the assumption $\partial p_1/\partial s > 0$. In the complementary case, $\partial p_1/\partial s < 0$, similar analysis gives the two band intensity equations

$$\frac{\partial I_1}{\partial s} - \frac{I_1}{p_1}\frac{\partial p_1}{\partial s} = -\Sigma_{T1}\left[I_1 - p_1 b\,\frac{acT^4}{4\pi}\right] \; , \tag{62}$$

$$\frac{\partial I_2}{\partial s} - \frac{I_1}{p_1}\frac{\partial p_2}{\partial s} = -\Sigma_{T2}\left[I_2 - p_2 b\,\frac{acT^4}{4\pi}\right] \; , \tag{63}$$

and the two band density equations

$$\frac{\partial \psi_1}{\partial s} = -\Sigma_{T1}[\psi_1 - b\,\frac{acT^4}{4\pi}] \ , \tag{64}$$

$$\frac{\partial \psi_2}{\partial s} + \frac{1}{p_2}(\psi_2 - \psi_1)\frac{\partial p_2}{\partial s} = -\Sigma_{T2}[\psi_2 - b\,\frac{acT^4}{4\pi}] \ . \tag{65}$$

The final item we consider is what happened at an interface between two dissimilar materials. We assume photons are flowing from left to right, and denote the band intensities just to the left of the interface by I_1^- and I_2^-. We wish to determine I_1^+ and I_2^+, the intensities just to the right of the interface. The underlying assumption we make is that the cross sections for the material to the left of the interface are uncorrelated from those for the material to the right of the interface. That is, the positions of the lines in one dissimilar material are uncorrelated to the positions of the lines in any other material. Then the photons in band I_1^- see both bands as they cross the interface, in proportion to the width of the bands on the plus side. The same is true, of course, for the photons in band 2. Hence all photons which cross the interface immediately populate the two bands on the plus side proportional to the widths of the plus side bands. We have

$$I_1^+ = (I_1^- + I_2^-)p_1^+ \ , \tag{66}$$

$$I_2^+ = (I_1^- + I_2^-)p_2^+ \ . \tag{67}$$

As an example of spatially dependent band parameters, we consider the steady state problem of a zero temperature slab (no re-emission) of thickness L with a perpendicular beam of radiation impinging upon the left boundary, and a vacuum at the right boundary. The radiation intensity will be non-zero only in the $\mu = 1$ direction, and hence

$$I(z,\nu,\mu) = I(z,\nu)\delta(1-\mu) \ , \tag{68}$$

where μ is the cosine of the angle between the photon flight direction and the positive z axis. The transport equation for $I(z,\nu)$ is

$$\frac{\partial I(z,\nu)}{\partial z} + \Sigma_T(z,\nu)I(z,\nu) = 0 \ . \tag{69}$$

We scale the frequency variable such that frequencies in the group of interest encompass $0 < \nu < 1$, and we assume a flat (in frequency) incident distribution, normalized to unity. The boundary condition on Eq. (69) is then

$$I(0,\nu) = 1 \ . \tag{70}$$

The cross section is assumed to have a two piece histogram behavior at any point z as shown in Figure 15. We measure distance such that the smaller opacity of the histogram has a value of unity. The heights unity and σ of the histogram are taken as independent of z, but the breakpoint between the two values varies with z, and is denoted by p(z) in the figure. We set

$$p(z) = z/L \tag{71}$$

as a concrete example.

For this problem, we compare the exact solution with the two band solution, as well as the one and two group Planck and Rosseland treatments. In particular, we compare the transmission through the slab, given by

$$T = \int_0^1 d\nu I(L,\nu) \ . \tag{72}$$

Since the problem is purely absorbing, the exact solution is easily obtained. Omitting the straightforward detail, the result is

$$T_{exact} = \frac{e^{-L} - e^{-\sigma L}}{(\sigma-1)L} \ . \tag{73}$$

In the two band treatment, it is clear how to choose the band parameters. We have

$$p_1 = z/L \; ; \quad p_2 = 1-z/L \; , \tag{74}$$

$$\Sigma_{T1} = 1 \; ; \quad \Sigma_{T2} = \sigma \; . \tag{75}$$

The two band equations are, assuming $\sigma > 1$ [see Eqs. (60) and (61)]

$$\frac{\partial \psi_1}{\partial z} + \frac{1}{z}(\psi_1 - \psi_2) + \psi_1 = 0 \; , \tag{76}$$

$$\frac{\partial \psi_2}{\partial z} + \sigma \psi_2 = 0 \; , \tag{77}$$

with boundary conditions

$$\psi_1(0) = \psi_2(0) = 1 \; . \tag{78}$$

The solution is

$$\psi_1(z) = \frac{1}{(\sigma-1)z}\left[e^{-z} - e^{-\sigma z}\right] \; , \tag{79}$$

$$\psi_2(z) = e^{-\sigma z} \; , \tag{80}$$

which leads to a transmission

$$T_{\text{two band}} = \frac{e^{-L} - e^{-\sigma L}}{(\sigma-1)L} \; . \tag{81}$$

Comparison of Eqs. (73) and (81) shows that the two band treatment gives the exact result for this example.

In contrast, the usual multigroup method using either Planckian or Rosseland means cannot give the exact result with a finite number of groups. For comparison, we have considered the one and two group results. Omitting the algebraic detail, the results are (the two group results correspond to two equal size groups):

$$T_{\text{one group-P}} = \exp[-L(\sigma+1)/2] \; , \tag{82}$$

$$T_{\text{one group-R}} = \exp\left[-\frac{\sigma L \ln \sigma}{(\sigma-1)}\right], \tag{83}$$

$$T_{\text{two group-P}} = \frac{1}{2}\{\exp[-(\sigma+3)L/4] + \exp[-(3\sigma+1)L/4]\} \quad , \tag{84}$$

$$T_{\text{two group-R}} = \frac{1}{2}\exp\left[-\frac{(\sigma-1+\sigma\ \ln\ \sigma)L}{2(\sigma-1)}\right]$$

$$+ \frac{1}{2}\exp\left[-\frac{(\sigma-1+\ \ln\ \sigma)\sigma L}{2(\sigma-1)}\right] . \tag{85}$$

Figures 16 through 18 plot Eqs. (82) through (85), ratioed to the two band (exact) result, as a function of slab thickness L for three different values of σ (2, 7, 20). It is clear from these results that one or two group Planckian or Rosseland calculations can be significantly inferior to a two band calculation. For this example, the latter is exact, although this is not true in general, of course. The error in the multigroup calculations becomes greater as σ increases, which is a manifestation that the problem is becoming increasingly non-gray as σ increases.

6. Concluding Remarks

The multiband method for spatially independent cross sections, as described in Sections 2 and 3, has been very successfully used in neutron transport calculations. Because of the strong similarity of the equation of radiative transfer to the neutron transport equation, one would expect the multiband method to be equally applicable to radiation flow problems. The extension of the method to spatially dependent cross sections, as described in Section 5 is a new idea which has not been fully developed nor tested numerically for any real problems. This extension should be particularly applicable to radiative transfer problems, but also has application in neutron transport (spatially dependent Doppler effects). We expect to explore this general formulation, and give numerical experience, diffusion theory formulations, Monte Carlo implementations, etc. in a future publication.

NOTICE

This report was prepared as an account of work sponsored by the United States Government. Neither the United States nor the United States Department of Energy, nor any of their employees, nor any of their contractors, subcontractors, or their employees, makes any warranty, express or implied, or assumes any legal liability or responsibility for the accuracy, completeness or usefulness of any information, apparatus, product or process disclosed, or represents that its use would not infringe privately-owned rights.

Reference to a company or product name does not imply approval or recommendation of the product by the University of California or the U.S. Department of Energy to the exclusion of others that may be suitable.

References

1. M. N. Nikolaev and V. V. Phillipov, At. Energ., 15, 493 (1963).

2. J. C. Stewart, JQSRT, 4, 723 (1964).

3. S. Glasstone and M. C. Edlund, The Elements of Nuclear Reactor Theory, Van Nostrand, New York (1962).

4. G. C. Pomraning, The Equations of Radiation Hydrodynamics, Pergamon Press, New York (1973).

5. D. E. Cullen, Nucl. Sci. Eng., 55, 387 (1974).

6. D. E. Cullen et al., "Cross Section Probability Tables in Multigroup Transport Calculations," UCRL-80655, Lawrence Livermore Laboratory, Livermore, California (1978).

7. C. R. Weisbin and R.J. La Bauve, "Specifications of Generally Useful Multigroup Structure for Neutron Transport," LA-5277MS, Los Alamos Scientific Laboratory, Los Alamos, New Mexico (1973).

8. P. R. Graves-Morris, ed., Pade Approximants and their Applications, pp. 217-240, Academic Press, New York (1973).

9. D. E. Cullen, "Definition of Two Band Parameters for Use in Photon Transport Calculations," UCID-17774, Lawrence Livermore Laboratory, Livermore, California (1978).

ACKNOWLEDGEMENT

This work was performed under the auspices of the U.S. Department of Energy by the Lawrence Livermore Laboratory under contract number W-7405-ENG-48. One of the authors (GCP) is grateful for the continued hospitality afforded him by the laboratory.

Table I

Weighting Functions for Photon and Neutron Transport		
Particles	Unshielded (Planckian)	Self-shielded (Rosseland)
Photons	$B_\nu(T)$	$\frac{1}{\Sigma_T} \frac{\partial B_\nu(T)}{\partial T}$
Neutrons	M(E)	$\frac{M(E)}{[\Sigma_T(E) + \Sigma_o]^N}$

Table II

Weighting Functions and Cross Sections in the Two-Band Treatment

$W(\Sigma_T)$	Cross Section
1	Planckian or unshielded
$1/\Sigma_T$	Rosseland or totally shielded
$1/\Sigma_T^2$	Super-Rosseland or totally shielded radiative flux (neutron current)

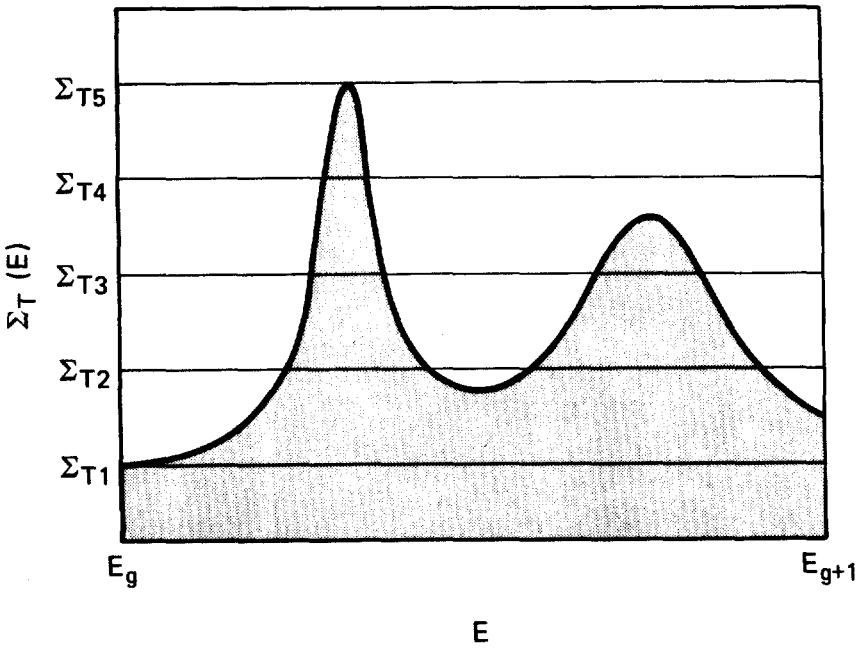

Fig. 1 Total Cross Section (4 cross section bands)

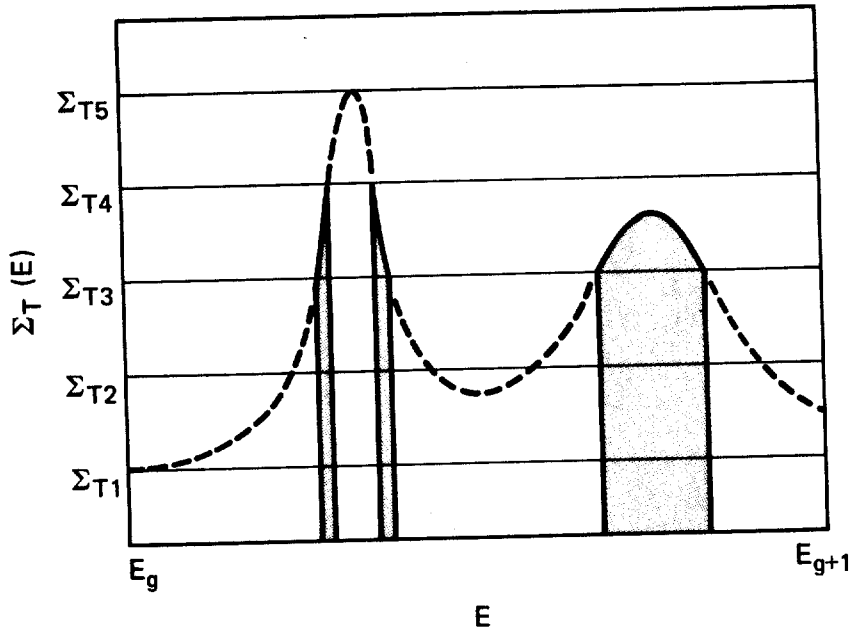

Fig. 2 Total Cross Section (Third band shaded)

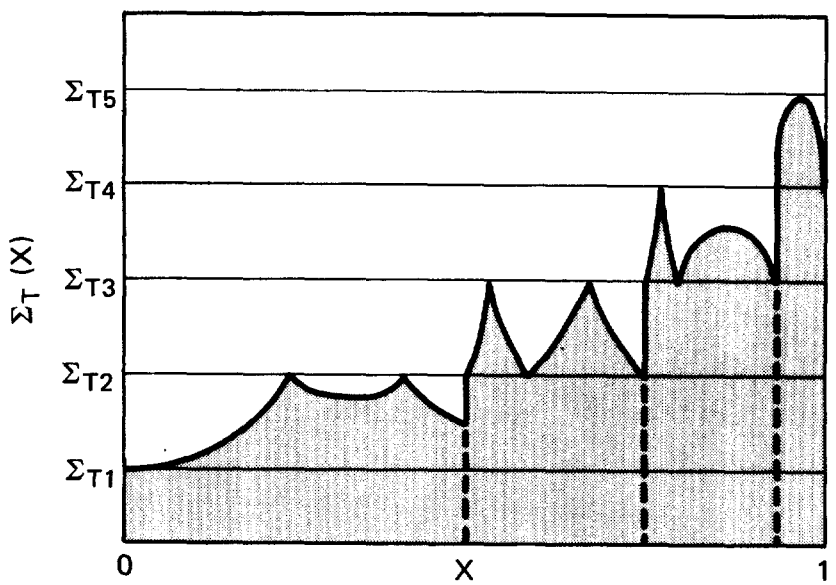

Fig. 3 Total Cross Section (Rearranged)

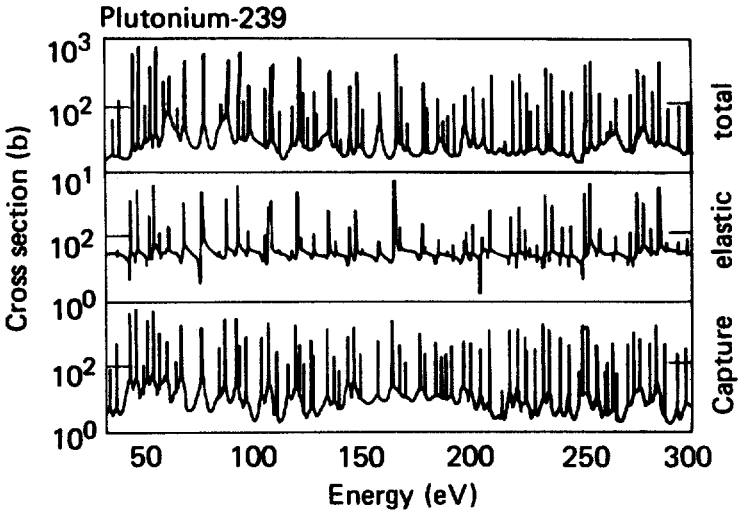

Fig. 4 Pu-239 Neutron Cross Section

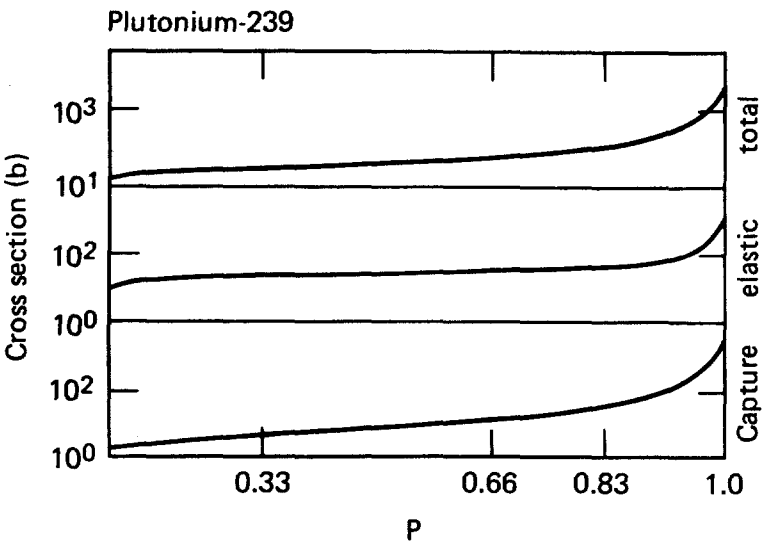

Fig. 5 Pu-239 Cumulative Cross Section Probability Distribution

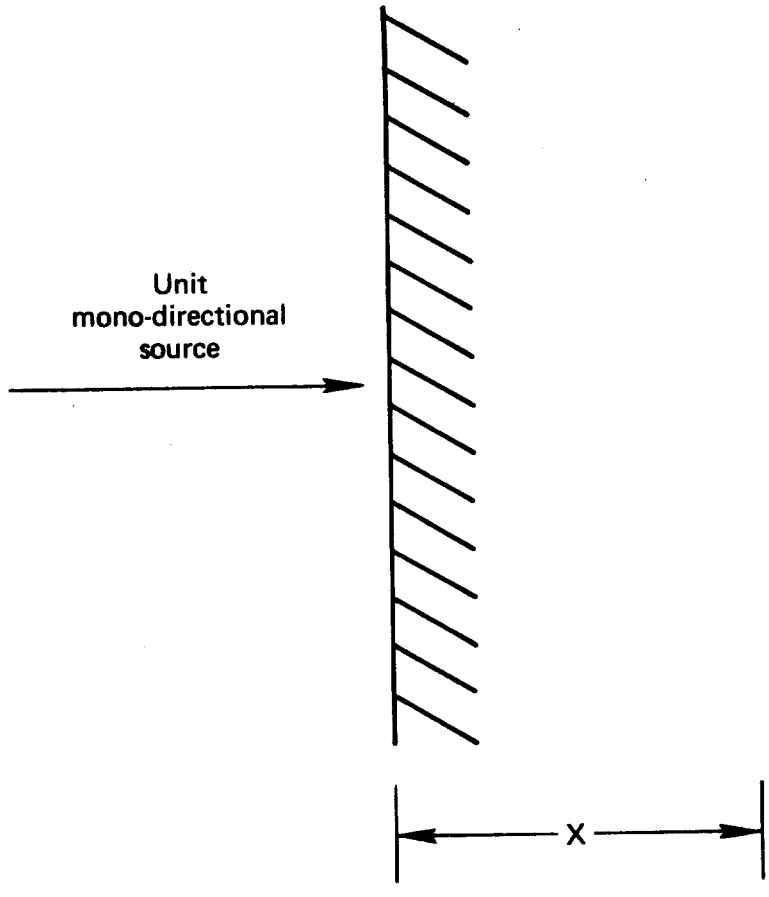

Fig. 6 Halfspace Geometry

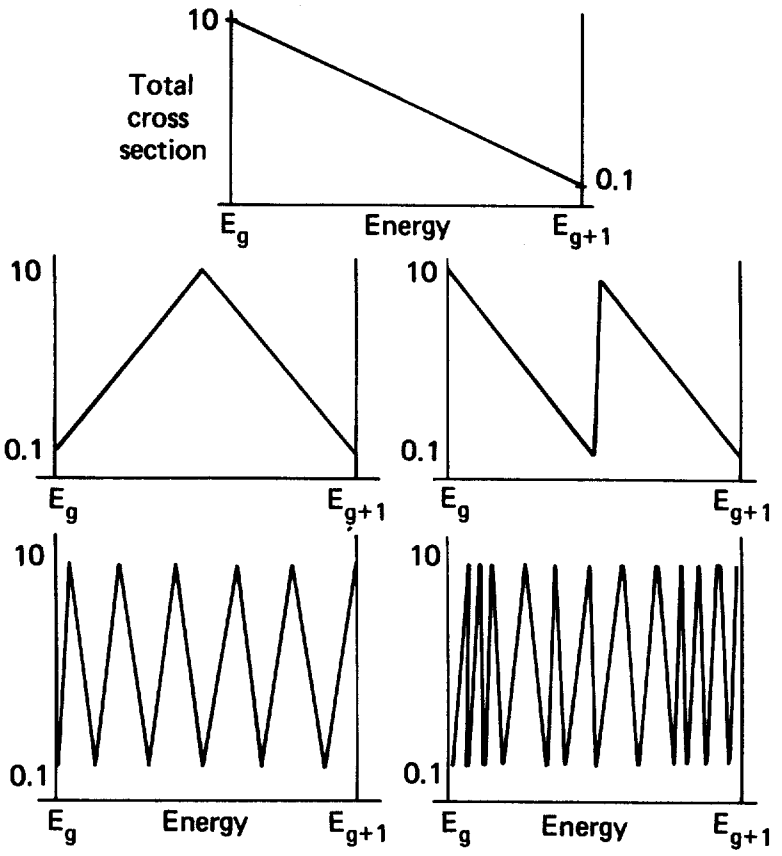

Fig. 7 Cross Sections Which Yield Identical Solutions

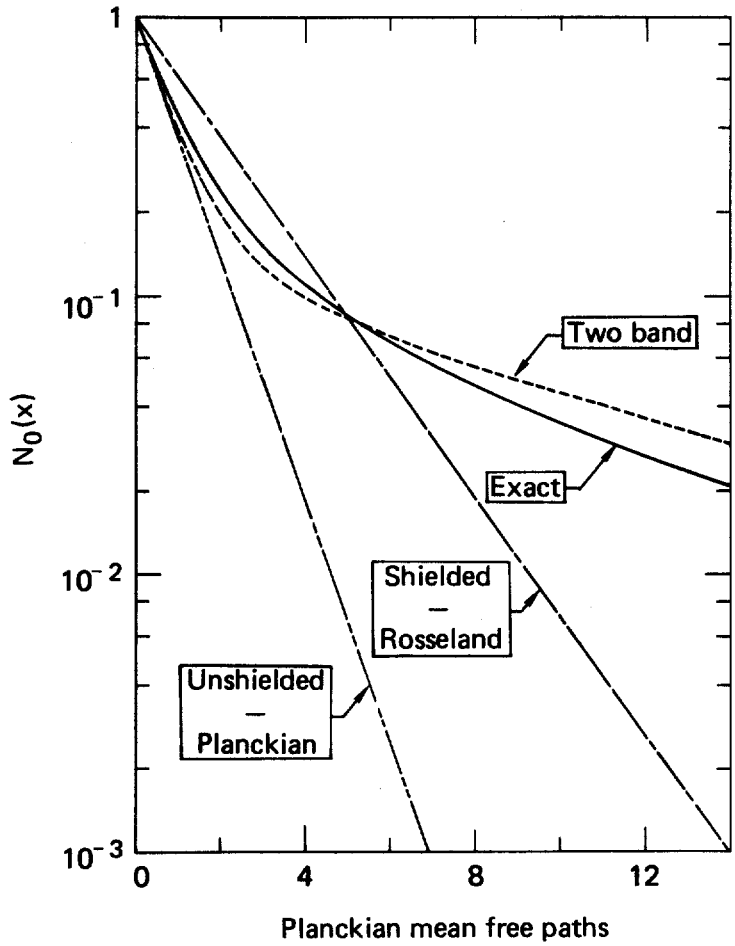

Fig. 8 Photon Intensity for Halfspace Problem

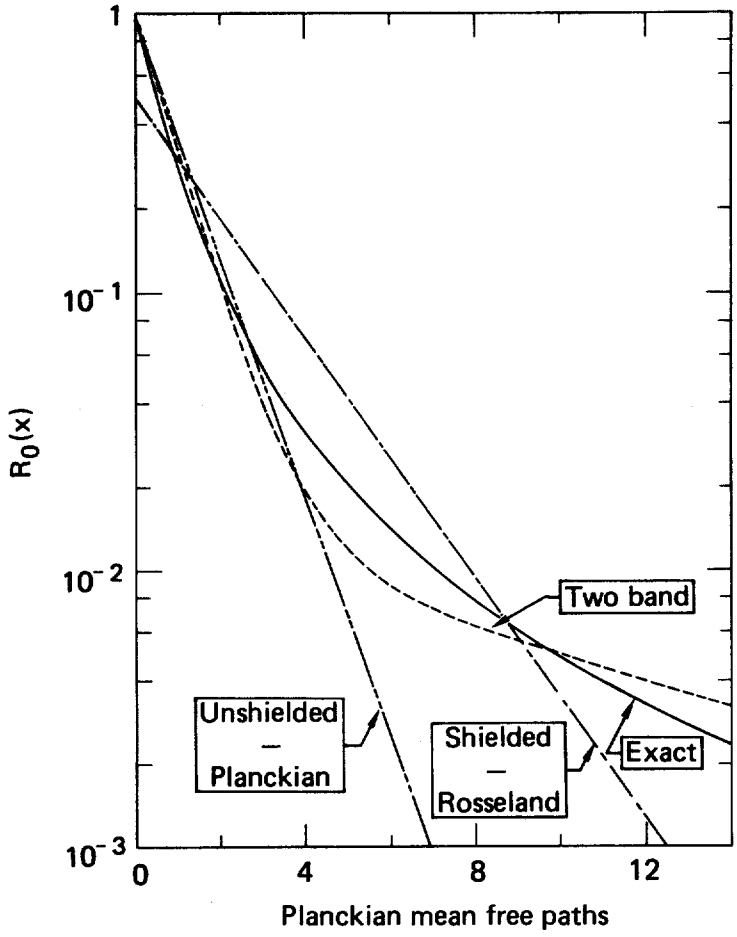

Fig. 9 Photon Reaction Rate for Halfspace Problem

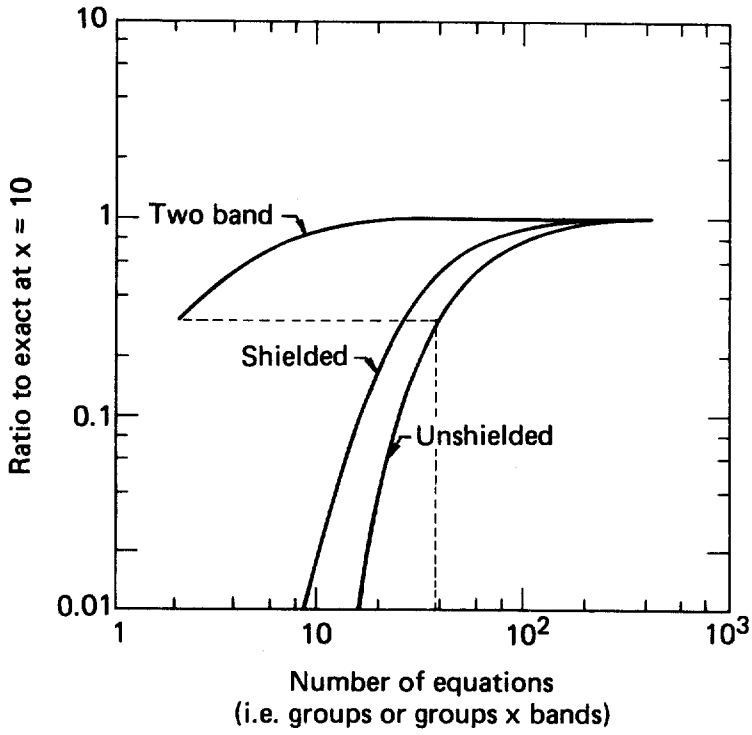

Fig. 10 Comparison of Multiband and Multigroup Results for Halfspace Problem

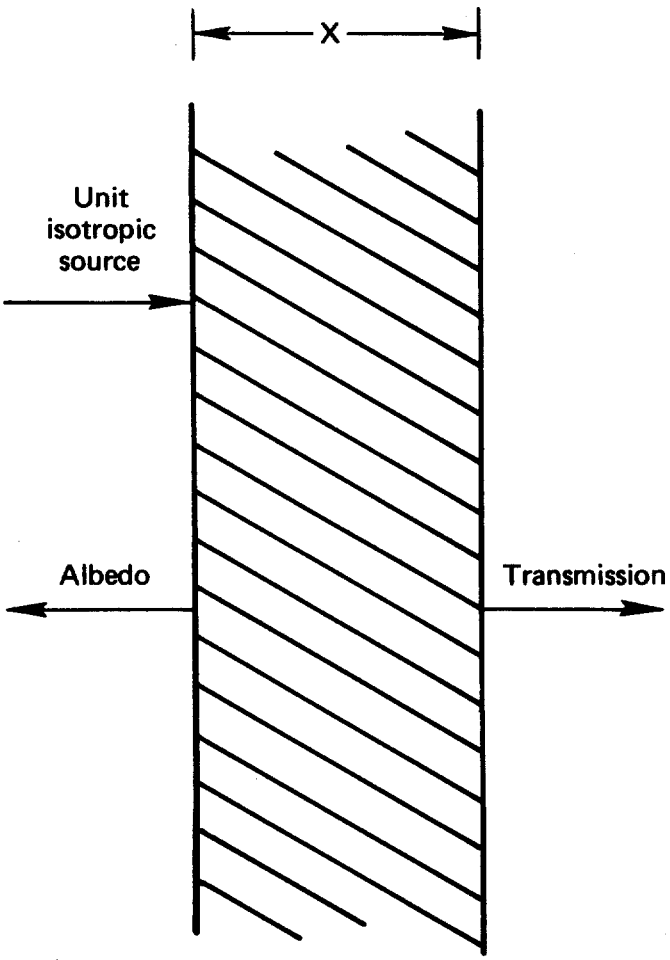

Fig. 11 Finite Slab Geometry

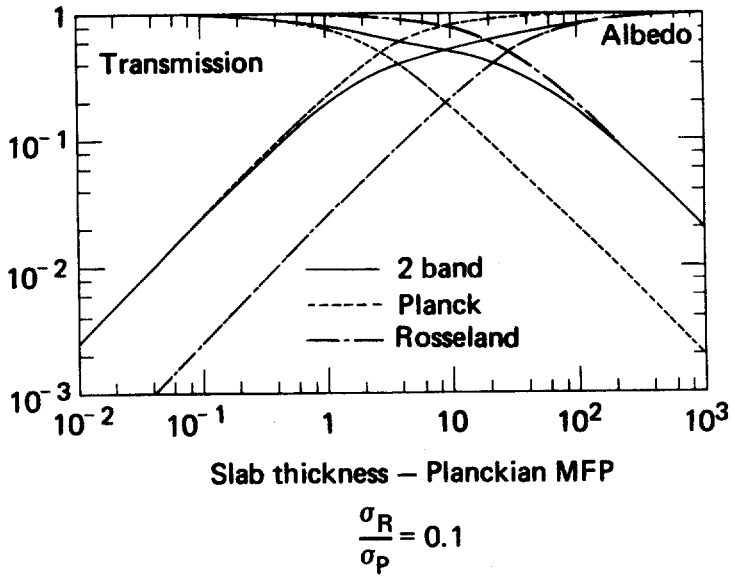

Fig. 12 Finite Slab Results

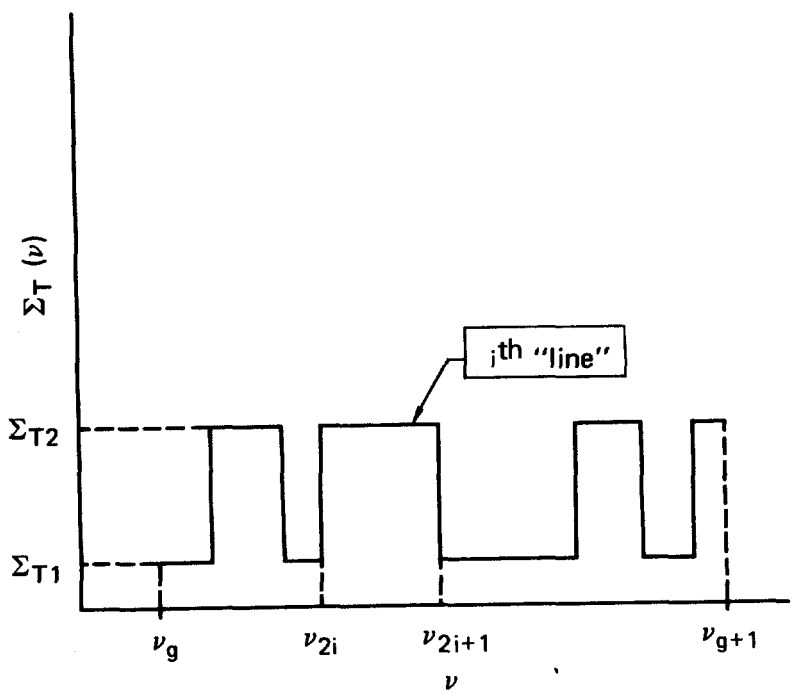

Fig. 13 Idealized Two Band Total Cross Section

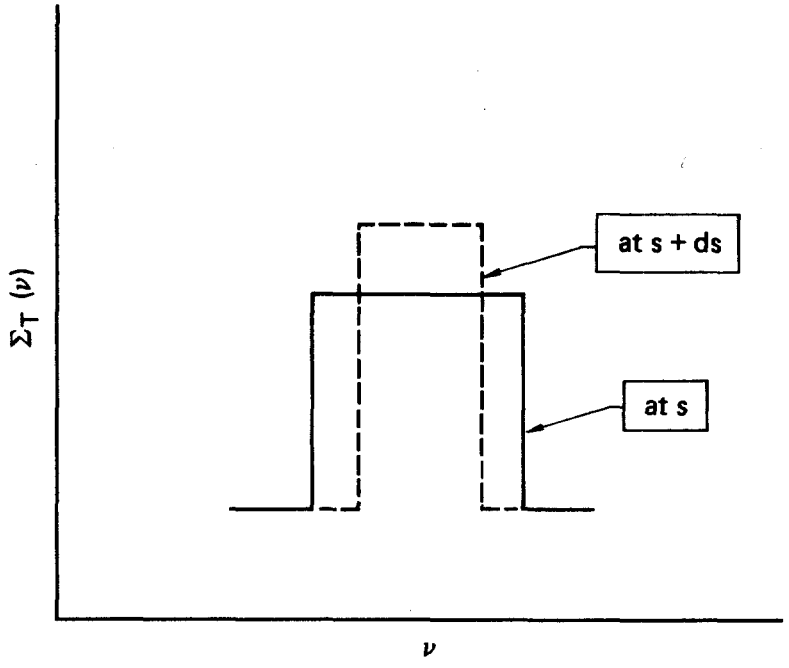

Fig. 14 An Idealized Single Line

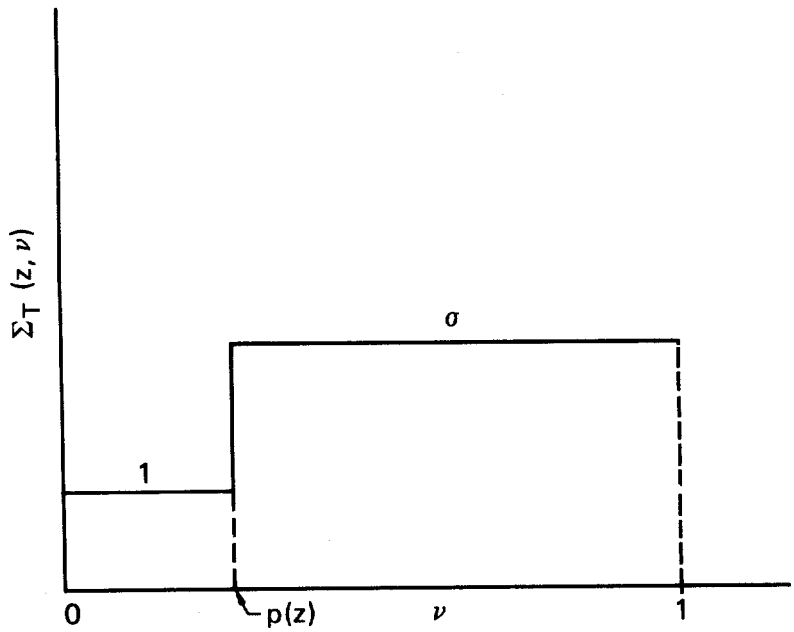

Fig. 15 A Model Cross Section

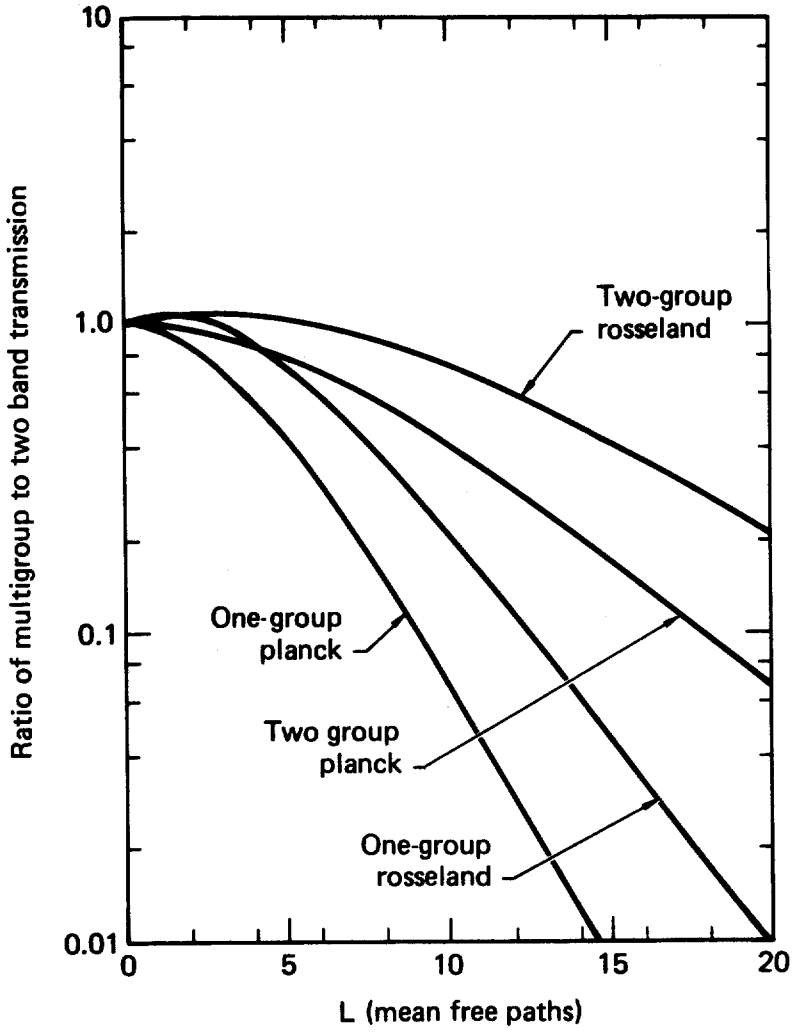

Fig. 16 One and Two Group Results for $\sigma = 2$

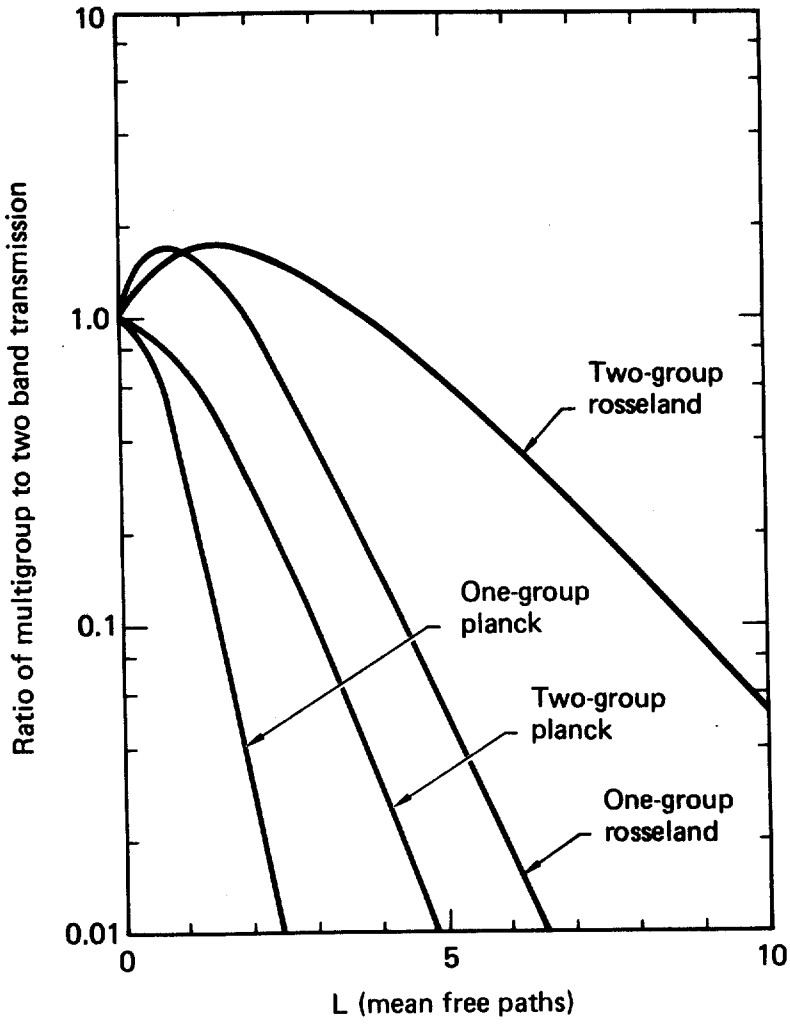

Fig. 17 One and Two Group Results for $\sigma = 7$

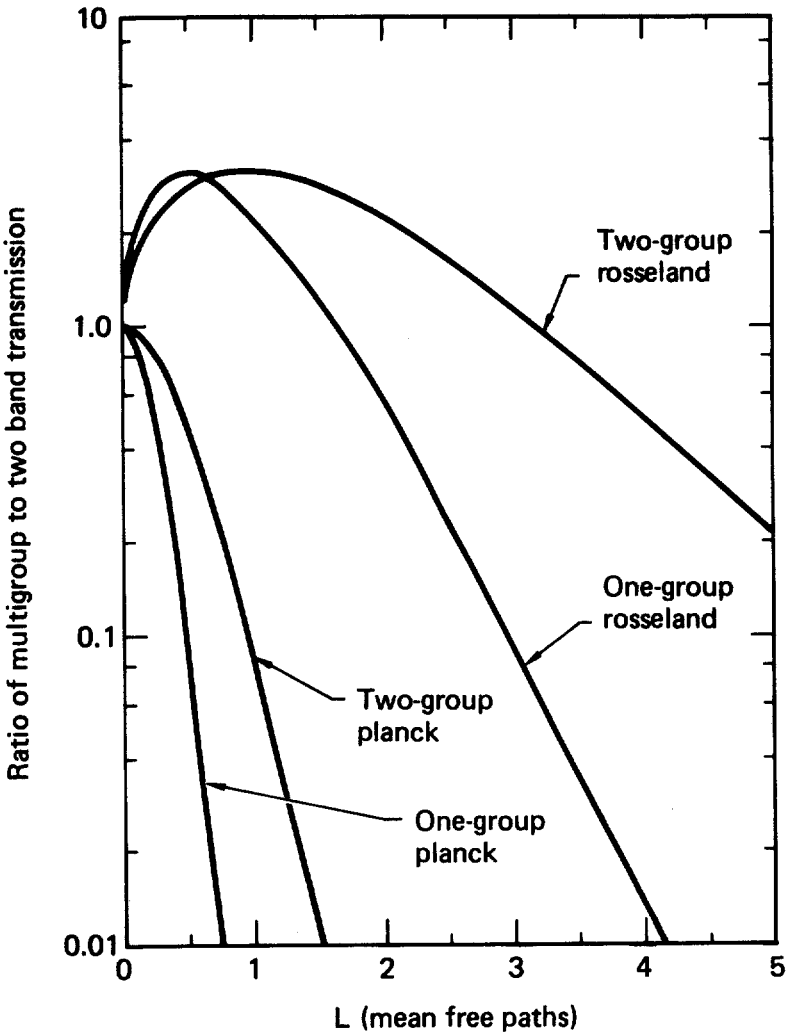

Fig. 18 One and Two Group Results for $\sigma = 20$

FIGURE CAPTIONS

Figure 1. Total Cross Section (4 cross section bands)

Figure 2. Total Cross Section (Third band shaded)

Figure 3. Total Cross Section (Rearranged)

Figure 4. Pu-239 Neutron Cross Section

Figure 5. Pu-239 Cumulative Cross Section Probability Distribution

Figure 6. Halfspace Geometry

Figure 7. Cross Sections Which Yield Identical Solutions

Figure 8. Photon Intensity for Halfspace Problem

Figure 9. Photon Reaction Rate for Halfspace Problem

Figure 10. Comparison of Multiband and Multigroup Results for Halfspace Problem

Figure 11. Finite Slab Geometry

Figure 12. Finite Slab Results

Figure 13. Idealized Two Band Total Cross Section

Figure 14. An Idealized Single Line

Figure 15. A Model Cross Section

Figure 16. One and Two Group Results for $\sigma = 2$

Figure 17. One and Two Group Results for $\sigma = 7$

Figure 18. One and Two Group Results for $\sigma = 20$